DYNAMIC ANALYSIS OF UNDERGROUND TUNNELS SUBJECTED TO INTERNAL BLAST LOADING

ROHIT TIWARI[1*], TANUSREE CHAKRABORTY[2], VASANT MATSAGAR[3]

[1]Graduate Student, Department of Civil Engineering,
Indian Institute of Technology (IIT) Delhi,
Hauz Khas, New Delhi - 110 016, India.
E-mail: rohit19862009@gmail.com.
[*]*Corresponding Author*

[2]Assistant Professor, Department of Civil Engineering,
Indian Institute of Technology (IIT) Delhi,
Hauz Khas, New Delhi - 110 016, India.
E-Mail: tanusree@civil.iitd.ac.in.

[3]Associate Professor, Department of Civil Engineering,
Indian Institute of Technology (IIT) Delhi,
Hauz Khas, New Delhi - 110 016, India.
E-Mail: matsagar@civil.iitd.ac.in.

Key words: *Blast Loading, Coupled Eulerian-Lagrangian Analysis, Finite Element Method, Strain Rate, Underground Tunnel.*

ABSTRACT

The present work deals with three dimensional nonlinear finite element (FE) analyses of underground tunnels in soil subjected to internal blast loading. The coupled Eulerian-Lagrangian (CEL) analysis tool in finite element software Abaqus/Explicit has been used for the analysis purpose. The soil and reinforced concrete lining has been modeled using the Lagrangian elements. The explosive TNT has been modeled using the Eulerian elements. The stress-strain response of soil, concrete and reinforcement has been simulated using strain rate dependent Drucker-Prager plasticity, concrete damaged plasticity and Johnson-Cook plasticity models, respectively. The pressure-volume relationship of TNT explosive has been simulated using the JWL equation-of-state. Parametric sensitivity studies have been performed for different (i) tunnel lining thicknesses, (ii) charge weights and (iii) friction angles of soil. It is observed from the results that pressure acting on the tunnel lining increases with the increase in charge weight. Both the lining and the surrounding soil undergo significant deformation. Deformation of the tunnel lining decreases with increasing lining thickness. Also, deformation of tunnel lining and soil decrease with increasing friction angle of soil.

1. INTRODUCTION

Underground tunnels used for roadway and railway, utility lines and water pipelines are indivisible part of the modern civil infrastructure. In the recent decades, explosion incidents caused by terrorist activities have proved to be a growing threat to the human civilization and the civil infrastructure. Internal explosion in a tunnel may lead to multiple reflections of the blast induced shock wave and thus channeling of the shock wave. Hence, in order to safeguard the tunnels, it is necessary to understand the response of these structures when subjected to blast. Experimental determination of the response of underground tunnels under blast loading often

becomes difficult due to socio-political issues. Thus, advanced numerical analysis of tunnels subjected to blast loading is of utmost importance.

In the literature, analyses on the effect of blast loading on underground structures have been carried out by many researchers. Chille et al. (1998) investigated the dynamic response of underground electric plant subjected to internal explosive loading using three dimensional numerical analysis methods. For traffic tunnels in rock mass, Choi et al. (2006) performed three-dimensional finite element (FE) analyses to study the blast pressure and resulting deformation in concrete lining. They found that the blast pressure on tunnel lining was not the same as the normally reflected pressure obtained using CONWEP (Department of the Army, the Navy, and the Air Force 1990). Lu et al. (2005) and Gui and Chien (2006) used FE procedure to perform blast analysis of tunnels subjected to external blast loading. Feldgun et al. (2008) used the variational difference method to analyze underground tunnels and cavities subjected to blast loads. Subway tunnels under explosive load have been analyzed by Liu (2009) using the FE method. Explosive load was modeled using CONWEP reflected pressure. The analysis performed by Liu did not consider the high strain rate behavior of soils under explosive loading. The effect of blast loading on tunnel considering the high strain rate behavior of soils has been studied in by Higgins et al. (2012). However, their study considered only elastic stress-strain response of concrete lining in the tunnel. The explosive was modeled using JWL equation-of-state. Chakraborty et al. (2013) compared the performance of different shock absorbing foam materials, steel and concrete tunnel linings under blast loading. The blast load was calculated through a coupled fluid dynamics simulation in their analyses. However, rigorous three dimensional simulations of lined underground tunnels in soil with properly simulated explosive load using JWL equation-of-state is rather unavailable in the literature due to the challenging nature of the problem.

The specific objectives of the present study are to perform three dimensional (3D) nonlinear finite element analysis underground tunnel subjected to internal blast loading and to understand the response of tunnel lining and surrounding soil when subjected to blast loading. The finite element (FE) analyses have been performed using the commercially available FE software Abaqus Version 6.11 (Abaqus manual version 6.11). Herein, finite element model of soil and reinforced concrete (RC) lining of the tunnel have been prepared using the Lagrangian analysis tool in Abaqus. Soil stress-strain behavior has been modeled using the Drucker-Prager constitutive model (Liu 2009). The RC lining has been modeled using the concrete damaged plasticity model (Chakraborty et al. 2013). The steel reinforcement is modelled using the Johnson-Cook (JC) plasticity (Johnson and Cook 1985) model. In case of blast loading the strain rate can reach upto 10^2 to 10^4 per second (Ngo and Mendis. 2008). Hence, strain rate dependent stress-strain response have been used for soil, steel and concrete. The TNT explosive and the surrounding air have been modeled using the Eulerian analysis tool in Abaqus. The pressure-volume relationship of the explosive is simulated using the Jones Wilkens Lee (JWL) (Zukas and Walters 2003) equation-of-state. Parametric sensitivity studies have been performed by varying (i) the concrete lining thickness (t_w), (ii) the weight of explosive (TNT) used and (iii) the angle of internal friction of soil (ϕ). The analysis results have been studied for stresses and deformation in soil and tunnel lining and damage of RC lining.

2 THREE DIMENSIONAL FINITE ELEMENT MODELLING

2.1 Lagrangian Finite Element Modelling of Soil and RC Concrete Lining

The three dimensional finite element model of the tunnel in soil has been developed using Abaqus with the Lagrangian analysis option. The FE mesh of the soil, tunnel lining, and reinforcement are shown in Figures 1(a) to 1(c). A 20 m long tunnel has been modeled in soil with reinforced concrete lining thickness of 350 mm with the center point of the tunnel at a minimum depth of 7.5 m from the ground surface. The reinforcement has been modeled with 10

mm and 12 mm diameter Fe415 bars in longitudinal and hoop reinforcement directions, respectively. The hoop reinforcement rings are placed at 250 mm center to center spacing. The longitudinal reinforcement bars are placed at a distance of 850 mm along inner arc. The distance between inner and outer hoop reinforcement is 120 mm. The 20 m long tunnel is placed in a soil domain of 20 m long, and 15 m × 15 m cross section. The FE models of the soil and RC lining geometry has been developed using the three dimensional part option in Abaqus/CAE using eight node reduced integration brick element with hourglass control and finite membrane strains (C3D8R). Mesh convergence and boundary convergence studies have been performed and higher mesh density has been used in tunnel lining and soil close to lining. The minimum element size in tunnel lining is considered 60 mm. The steel reinforcement has been embedded in tunnel lining and modeled using the two node beam elements (B31). Proper bonding between concrete and reinforcement bars has been assured by applying embedded region constraints option available in Abaqus. The bottom plane of the soil domain has been fixed in all Cartesian directions, *x*, *y* and *z*. The vertical side planes and the front and back side planes of the soil domain and tunnel lining have been provided with pinned support as detailed in Figure 1 by constraining the normal displacements perpendicular to the plane (U) and the out-of-plane rotations (U_R). The contact between tunnel lining and soil has been modeled with the general contact option in Abaqus with hard contact in the normal direction and frictionless contact in the tangential direction.

2.2 Eulerian Finite Element Modelling of Explosive

The explosive material has been modeled using the Eulerian modeling technique in Abaqus. Figure 1(d) shows a typical FE mesh of explosive. To model Eulerian explosive material and the surrounding air domain inside the tunnel, Eulerian continuum three dimensional eight node reduced integration elements (EC3D8R) have been used. The Eulerian and Lagrangian elements can interact with each other through the general contact defined between explosive, air and tunnel lining surface. Free outflow boundary condition has been defined at the boundary of air domain, thus, blast pressure when reaches boundaries of air domain, it propagates freely out of the air domain without any kind of reflection. A fine mesh of Eulerian elements is necessary to efficiently capture the propagation of blast wave through air, the surrounding concrete lining and the soil. Mesh convergence study has been performed in the present study to decide the smallest element size as 35 mm. The pressure-volume relation of explosive has been simulated using Jones Wilkens Lee (JWL) equation-of-state. In this model, the pressure (P_s)-volume (v) relationship can be represented as the sum of functions given by

$$P_s = Ae^{-R_1 V} + Be^{-R_2 V} + C\left[\frac{v}{v_0}\right]^{-(1+\omega)} \quad (1)$$

where v_0 is the initial specific volume of explosive material. The parameters A, B, C, R_1, R_2 and ω are material constants in which A, B and C have dimensions of pressure and rest of the constants are dimensionless. In JWL equation of state, the first two exponential terms are high pressure terms and the last term on the right hand side is a low pressure term which deals with the high volume of cloud due to explosion. The material properties used herein for JWL has been listed in Table 1 as obtained from Zukas and Walter (2003) and Abaqus manual version 6.11.

3 MATERIAL PROPERTIES

3.1 Mateial Properties for Concrete

The concrete in tunnel lining has been modelled as M30 grade (ultimate compressive strength of 30 MPa) using the concrete damage plasticity model in Abaqus. The yield function in the concrete damaged plasticity model is given by Lubliner et al. (1989). The elastic properties of concrete are listed in Table 2. For concrete, modulus of elasticity E_s = 27.4 GPa, compressive strength of concrete f_{ck} = 30 MPa, mass density ρ = 2400 kg/m^3 and Poisson's ratio ν = 0.2 have

been considered. Figures 2(a) and 2(b) show the stress-strain curves for M30 concrete in compression and tension, respectively (Carreira and Chu 1985, 1986). Similarly, Figures 2(c) and 2(d) show the damage-strain curves for M30 concrete in compression and tension, respectively (Carreira and Chu 1985, 1986). For strain rate dependent material properties, dynamic increase factors (DIF) of 2.1 and 6 have been used for compressive and tensile stress-strain responses, respectively at 100/sec strain rate (Bischoff and Perry 1991).

3.2 Material Properties for Steel

The stress-strain behavior of steel reinforcement has been modelled using Johnson-Cook (JC) model (Johnson and Cook 1985). The Fe 415 grade of steel has been considered for the lining reinforcement. The elastic material properties of steel are given in Table 2. For steel, modulus of elasticity E_s= 200 GPa, tensile yield strength f_y= 415 MPa, mass density ρ = 7800 kg/m^3 and Poisson's ratio ν = 0.3 have been considered. For strain rate dependent modeling as per JC model, the material constants are obtained from mechanical testing and adopted herein for strain rate of 100/sec, as, A = 360 MPa, B = 635 MPa, n = 0.114, C = 0.075. These values are computed based on tensile test data of the material as per the JC model (Goel et al. 2011). The effect of temperature on JC model has been neglected herein.

3.3 Material Properties of Soil

The soil surrounding the tunnel has been modeled using the Drucker Prager plasticity model. Here, linear Drucker Prager criteria has been used in the modelling of soil which provides a noncircular yield surface in the deviatoric plane to match different yield values in triaxial tension and compression. A non-associated flow rule is considered in the present analysis by considering the dilatancy angle of sand to be different from the friction angle. The material properties used for sand are given in Table 3. For sand, modulus of elasticity E_{soil} = 28 MPa, mass density ρ = 1560 kg/m^3, Poisson's ratio ν = 0.2, friction angle ϕ = 30° and dilation angle ψ = 5° have been considered. The strain rate dependent stress-strain response of sand has been obtained from Veyera and Ross (1995).

4. TYPES OF ANALYSES

The numerical simulations have been performed for two RC lining thicknesses - 350 mm and 550 mm for 50 kg TNT explosive and 30° friction angle of sand. Parametric studies have been performed for three different charge weights of 25 kg, 50 kg and 100 kg for 350 mm lining thickness and 30° friction angle of sand. Analyses have also been carried out for three different angles of friction - 25°, 30°, 35° for 50 kg charge weight and 350 mm lining thickness. The analyses have been performed in a single dynamic explicit step. Gravity loading has been applied. For studying the response of the complete 20 m tunnel section, the duration of analysis is maintained such that the shock wave can travel through the complete tunnel length. Analysis duration of 16 msec has been maintained in all simulations.

5. VALIDATION OF FINITE ELEMENT ANALYSIS

To ensure the validity of the numerical simulations, the results of CEL simulation for blast loading on a concrete slab has been compared with the results where blast loading is simulated using TM5-1300. A 1.2 m × 1.2 m × 0.09 m reinforced concrete (RC) slab has been analyzed numerically using the CEL method. The slab is subjected to a blast loading caused by 1.69 kg TNT charge weight at three different scaled distance of 0.5, 1.0, 5 m/kg$^{1/3}$. In CEL, TNT explosive has been simulated using JWL equation-of-state. The boundaries of the concrete slab are restrained in three Cartesian directions, e.g., x, y and z. In another analysis, the blast load has been calculated using TM5-1300 (Departments of the Army and Navy and the Air Force 1990) and the modified Friedlander's equation (Goel et al. 2012) for the same charge weight and scaled

distances as mentioned above. Figure 3 shows the comparison of central node displacement calculated through CEL simulation and the simulation using TM5-1300. It is clearly seen from the figure that both the results compare with reasonable accuracy.

6. RESULTS AND DISCUSSION OF PARAMETRIC STUDIES

Parametric sensitivity studies of an underground tunnel in soil has been carried out for different (i) concrete lining thickness (t_w), (ii) weight of explosive (TNT) used and (iii) angle of internal friction of soil mass (ϕ). Figure 4 shows the paths in the tunnel along which the results are extracted. It may be noted that for minimizing the boundary effect only central 10 m path length has been considered for extracting the results.

6.1 Variation of RC Lining Thickness

Figures 5 (a) and 5(b) show the displacement of reinforced concrete lining along two paths - one along tunnel crown and the other along tunnel sidewall, for 350 mm and 550 mm RC lining thicknesses at 16 msec for 50 kg TNT charge weight. Higher displacement is observed in the 350 mm lining along both tunnel crown and sidewall which may be attributed to higher damage of the 350 mm tunnel lining when subjected to blast loading as compared to the 550 mm tunnel lining. The displacement is negative at the crown and positive at the side wall which signifies that the tunnel crown moves downward and the left sidewall moves inward under blast loading. The 550 mm lining exhibits almost 90% lesser displacement as compared to the 350 mm lining. The deformed shape of the tunnel cross section is inserted in Figure 5(c). Figure 5(c) shows the displacement time history at the tunnel crown in the lining just above the explosive. For both the lining thicknesses, displacement along tunnel crown increases with time. Higher displacement is observed for 350 mm thick lining as compared to the 550 mm thick lining which is reasonable. Figures 5(d) and 5(e) show the displacement of soil along the crown and the left side wall surrounding the RC lining. Irregular displacement pattern is observed in soil for 350 mm tunnel lining due to complete damage of the lining. The 550 mm lining exhibits comparatively lesser damage which is expected. Figure 5(f) shows the displacement time history of soil at the tunnel crown. At tunnel crown, soil exhibits almost 40% lesser displacement when 550 mm lining is used as compared to that for 350 mm lining. Figure 6 shows the displacement at 250 mm inside soil from the tunnel lining and along a path from tunnel crown. High displacement in soil is observed even at 250 mm away from the lining. Up to 250 mm, the shock wave pushes tunnel lining and soil together. However, above 250 mm, the soil moves downward under gravity. Hence, the displacement is positive for the first 250 mm and then negative.

6.2 Variation of Charge Weights

Figures 7(a) and 7(b) show the displacement response at the tunnel crown and the left side wall for three different charge weights of 25 kg, 50 kg, 100 kg. Higher displacement is observed for 100 kg charge weight as compared to 25 kg charge weight which is expected. It may be however noted that at tunnel crown, 50 kg explosive produces highest displacement whereas at tunnel sidewall, 100 kg explosive produces the maximum displacement which may be attributed to irregular damage pattern of the tunnel wall when subjected to blast loading. For 50 kg explosive, almost 75% higher displacement at tunnel crown is observed as compared to 25 kg explosive. Figure 7(c) shows displacement time history plot at tunnel crown. The displacement at the crown increases with increasing time for all charge weights. Figures 7(d) and 7(e) show the displacement response in soil both at the crown and at the sidewall. In both the cases, higher displacement is observed for 100 kg charge weight as compared to that for 25 kg charge weight. However, for 50 kg charge weight, more noise in displacement response is observed. Almost 78% higher displacement is observed in soil for 50 kg explosive as compared to that for 25 kg explosive. Figure 7(e) shows displacement time history plot in soil. The displacement in the soil increases with increasing time for all charge weights.

6.3 Variation of Soil Friction Angle

Figures 8(a) and 8(b) show the deformation of RC lining for the paths along the tunnel crown and the left sidewall for three different angle of friction of soil - 25°, 30°, 35°. The results show clearly that the deformation of the lining decreases with increasing angle of friction. In tunnel lining, almost 23% and 56% lesser displacement is exhibited for $\phi = 35^\circ$ as compared to that for $\phi = 30^\circ$ and $\phi = 25^\circ$. Figure 8(c) shows the time history of deformation at the tunnel crown. Here also, the deformation decreases with increasing friction angle. Thus, sands with higher friction angle may be used in blast resistant design of tunnels underground. Figures 8(d) and 8(e) show the deformation in soil. Soil deformation decreases significantly for 30°, 35° friction angles as compared to that for 25° friction angle. In soil, almost 38% and 60% lesser displacement is exhibited for $\phi = 35^\circ$ as compared to that for $\phi = 30^\circ$ and $\phi = 25^\circ$. Figure 9 shows the displacement contour in soil for different soil friction angles. Maximum influence zone for displacement is observed in soil with 25°friction angle.

7. CONCLUSIONS

In the present study, three dimensional nonlinear finite element (FE) analyses of underground tunnels in soil subjected to internal blast loading have been carried out. The coupled Eulerian-Lagrangian (CEL) analysis tool in finite element software Abaqus/Explicit has been used for the analysis purpose. The explosive TNT has been modeled using the Eulerian elements. The stress-strain response of soil, concrete and reinforcement has been simulated using strain rate dependent Drucker-Prager plasticity, concrete damaged plasticity and Johnson-Cook plasticity models, respectively. The pressure-volume relationship of TNT explosive has been simulated using the JWL equation-of-state. Parametric sensitivity studies have been performed for different (i) tunnel lining thicknesses, (ii) charge weights and (iii) friction angles of soil. It has been concluded from the analyses that blast induces damage in tunnel lining decreases with increasing lining thickness. The 550 mm lining exhibits almost 90% lesser displacement as compared to the 350 mm lining. Lining and soil displacement increases with increasing charge weight. Almost 78% higher displacement is exhibited in soil for 50 kg explosive as compared to that for 25 kg explosive. The displacement in the soil increases with increasing time for all charge weights. Lining and soil displacement decreases with increasing friction angle of soil. In soil, almost 38% and 60% lesser displacement is exhibited for $\phi = 35^\circ$ as compared to that for $\phi = 30^\circ$ and $\phi = 25^\circ$.

TABLES

Table 1 JWL material properties for TNT explosive

Density (ρ) (kg/m^3)	Detonation Wave Speed (V) (m/sec)	A (MPa)	B (MPa)	ω	R_1	R_2	Detonation Energy Density (ρ_d) (J/kg)
1630	6930	373800	3747	0.35	4.15	0.9	3680000

Table 2 Concrete and steel material properties

Material	Yield Strength (f_y) (MPa)	Elastic Modulus (E_c) (GPa)	Poisson's Ratio (ν)	Strain Rate
Concrete (M30)	30	27.4	0.2	100/Sec
Steel (Fe415)	415	200	0.3	100/Sec

Table 3 Ottawa sand material properties

Density (ρ) (kg/m^3)	Elastic Modulus (E_{soil})	Poisson's Ratio (ν)	Friction angle (ϕ)	Dilation angle (ψ)	Strain rate
1560	28 (MPa)	0.2	30°	5°	1000/sec

FIGURES

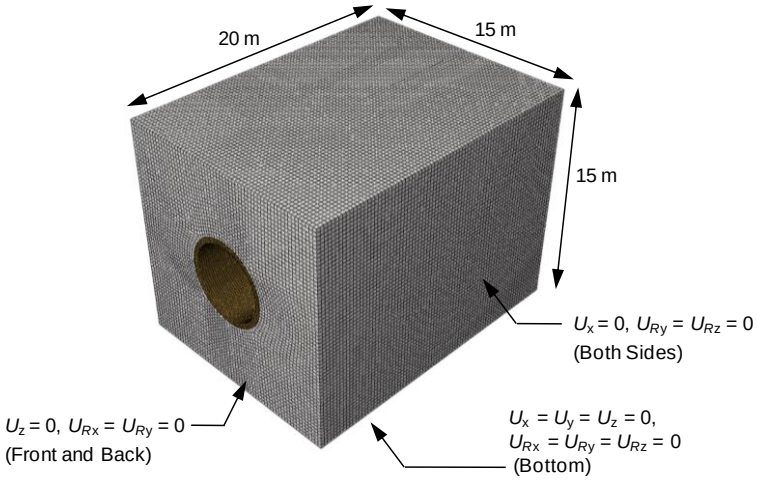

(a) Tunnel with reinforced concrete lining in soil

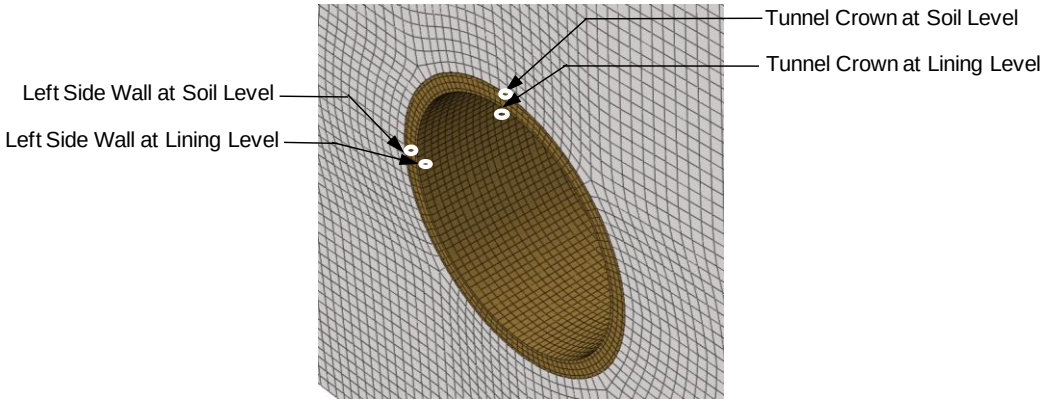

(b) Enlarged mesh with geometrical detailing

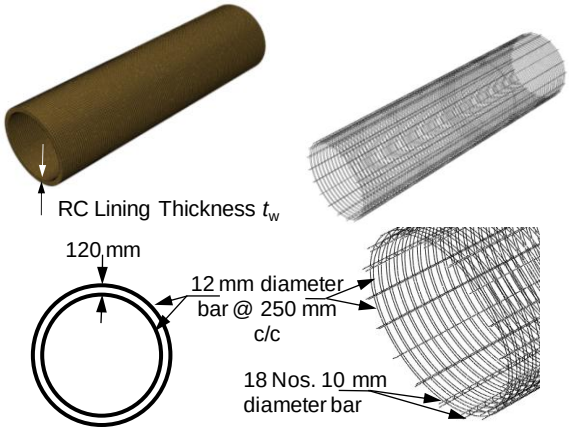

(c) Reinforcement details

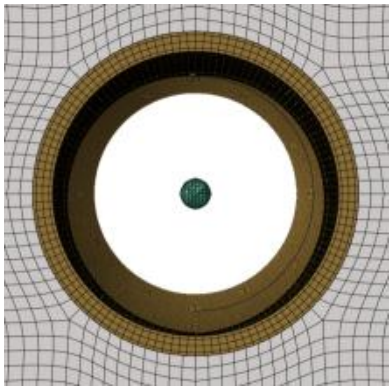

(d) Explosive inside tunnel

Figure 1: Tunnel geometry and reinforcement details.

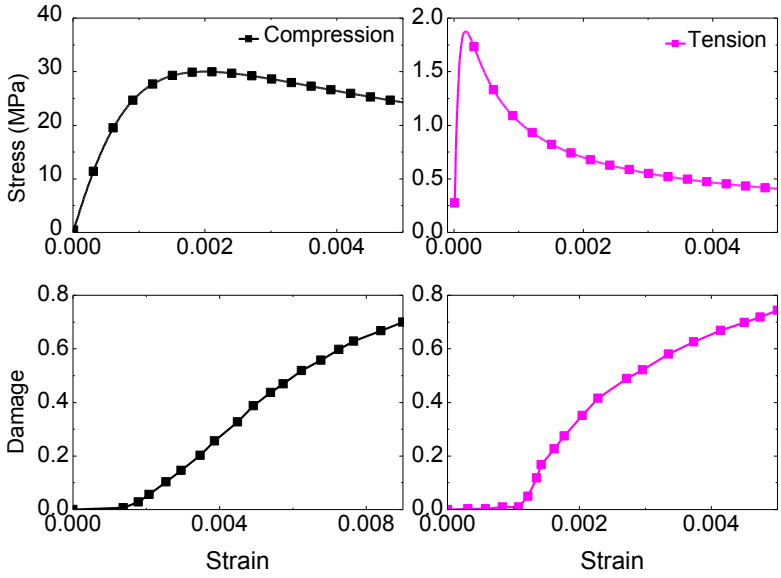

Figure 2: Stress-strain and damage-strain curves for M30 grade of concrete in compression and tension (Carreira and Chu 1985, 1986).

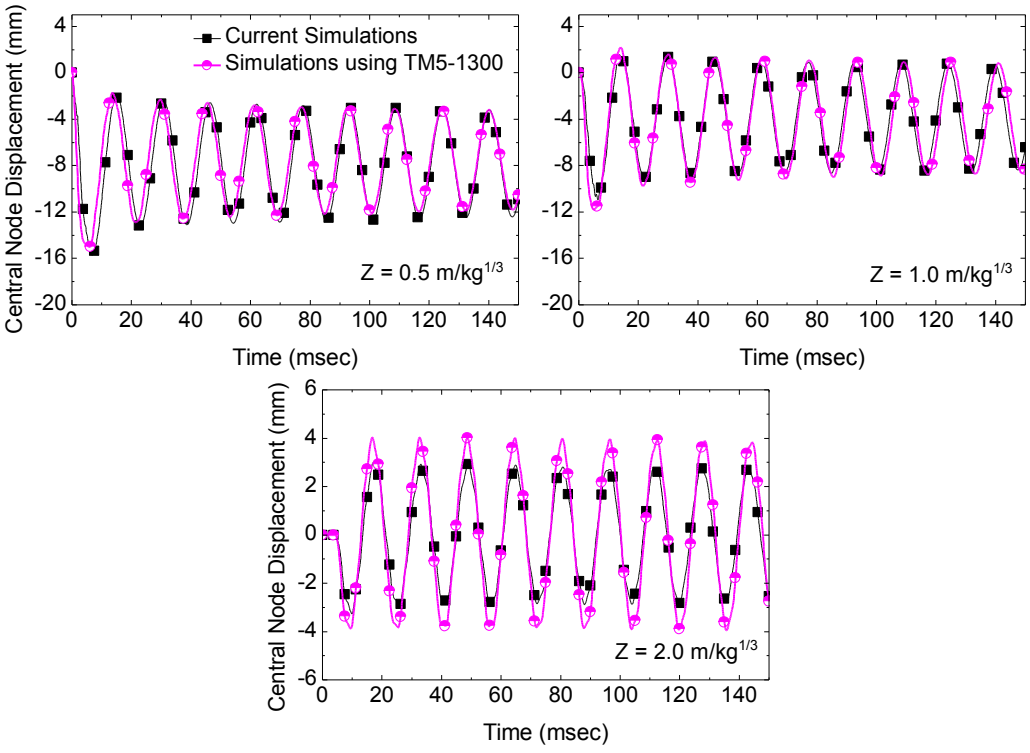

Figure 3: Comparison of central node displacement time histories for simulations using CEL and TM5-1300.

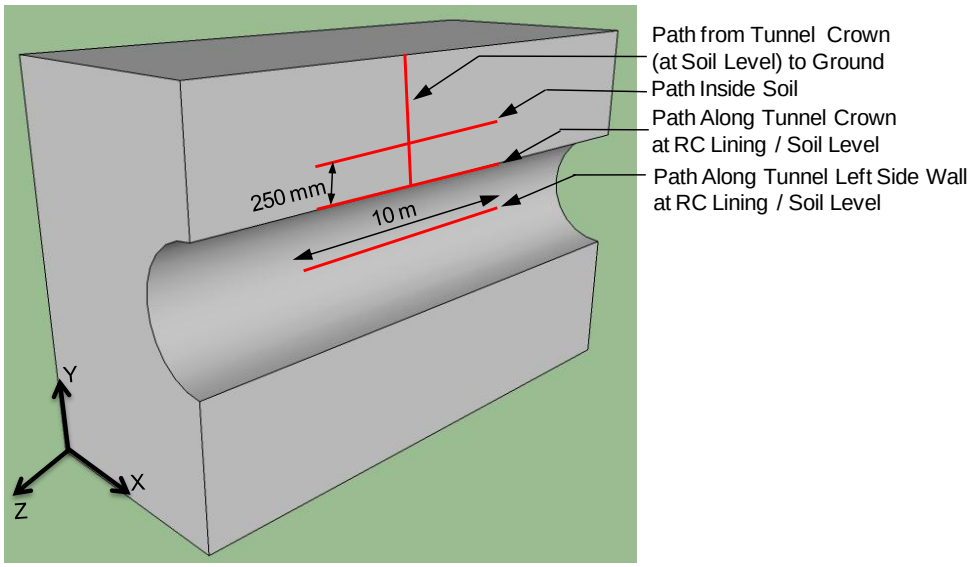

Figure 4: Paths defined for visualization.

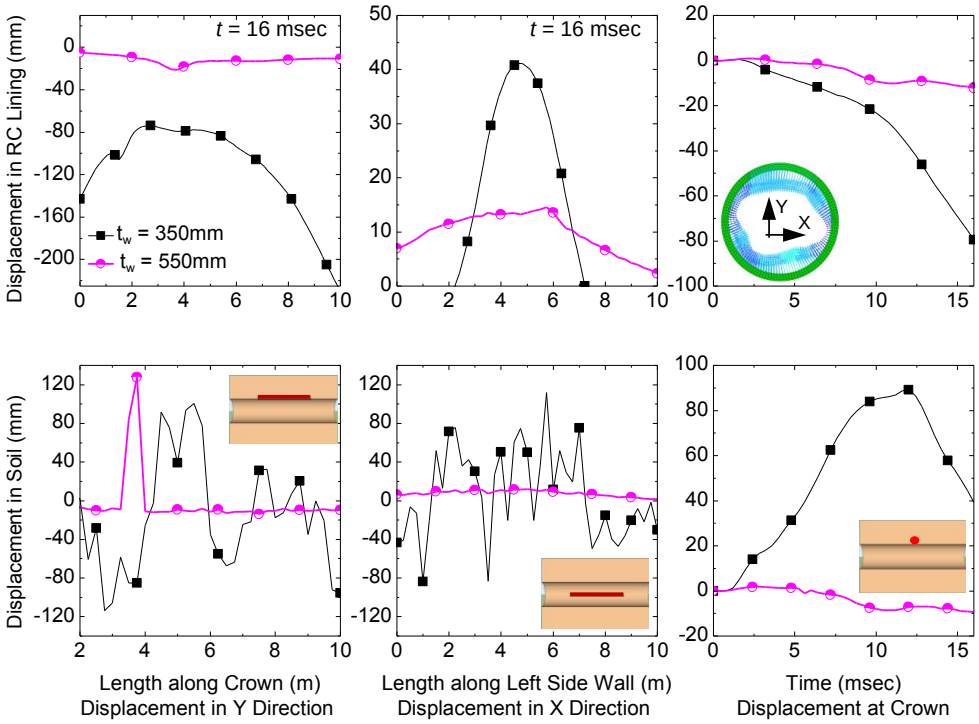

Figure 5: Displacement of RC lining and soil for different lining thicknesses.

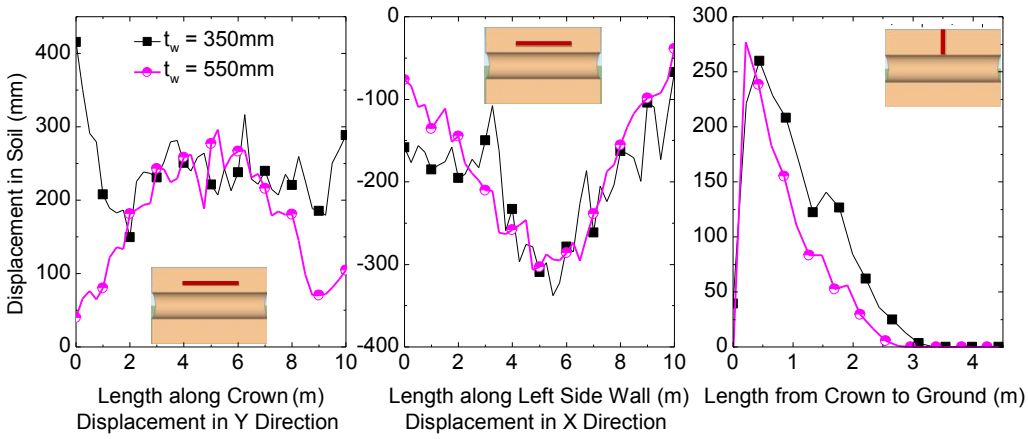

Figure 6: Displacement in soil 250 mm away from the lining at crown and left side wall for different lining thicknesses at 16 msec.

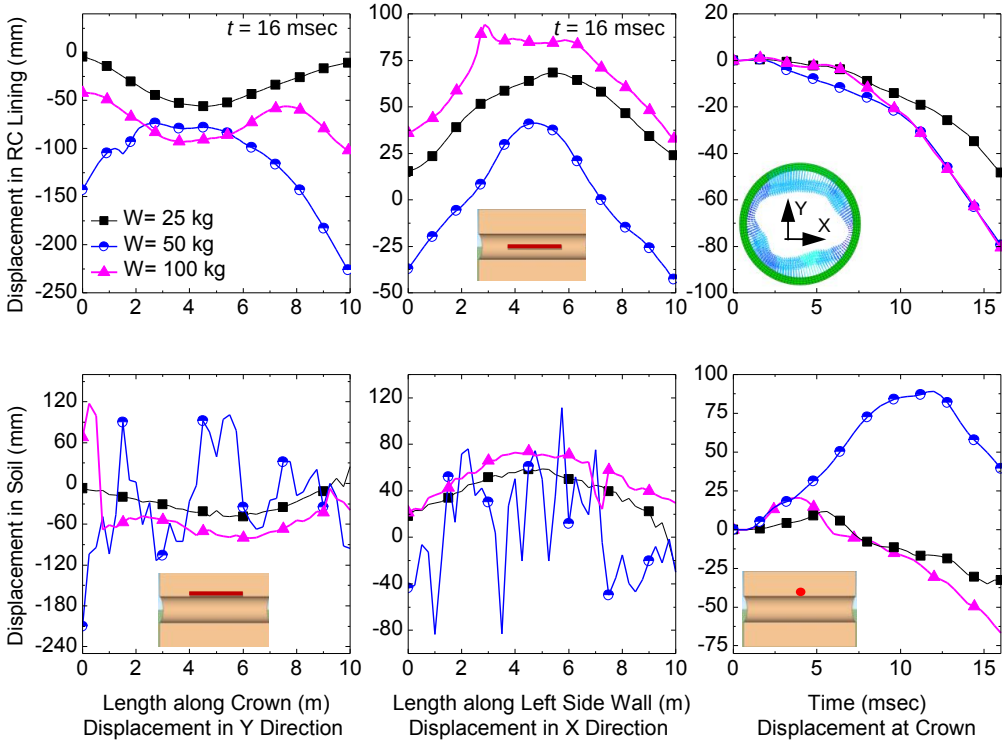

Figure 7: Displacement of RC lining and soil for different charge weights.

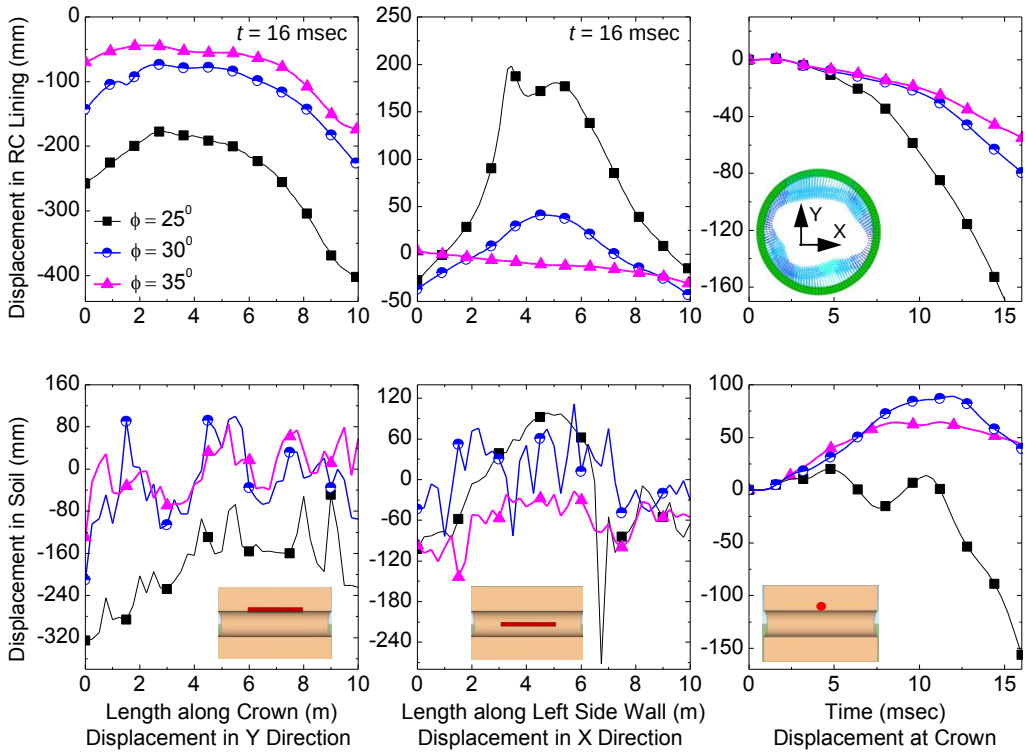

Figure 8: Displacement of RC lining and soil for different soil friction angles.

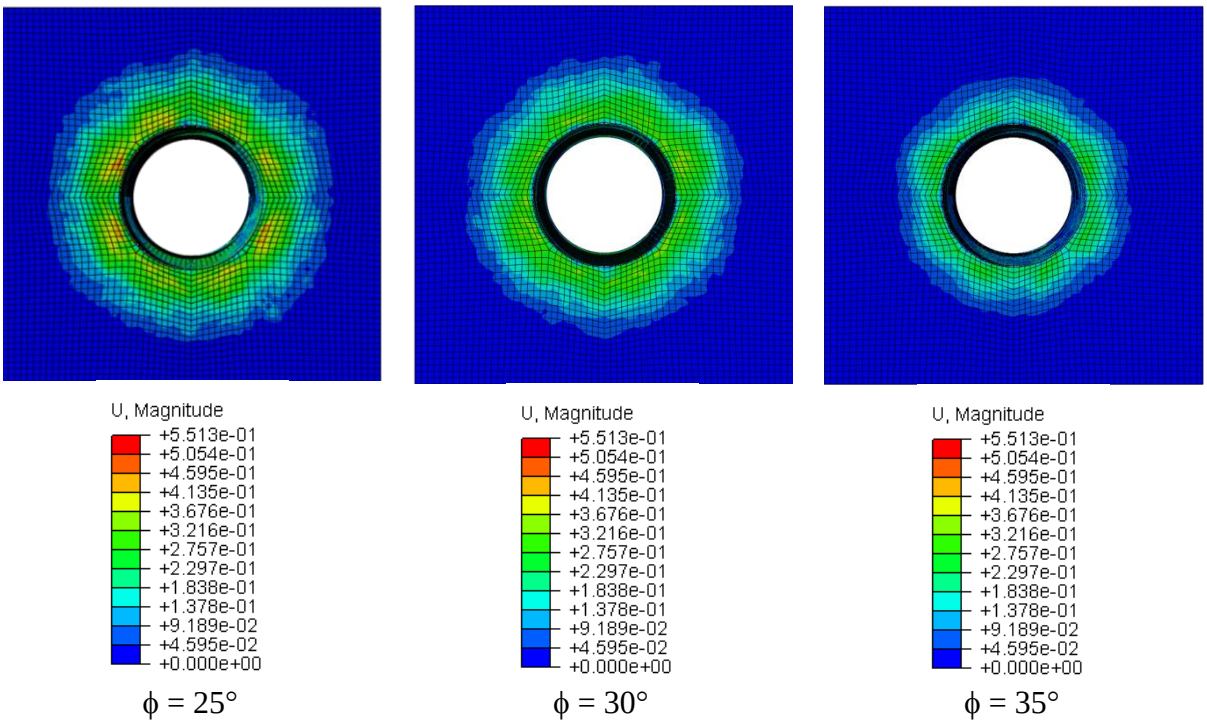

Figure 9: Deformation contour in soil for different friction angles at 15 msec, for 50 kg charge weight and 350 mm lining thickness.

REFERENCES

[1] Abaqus/Standard User's Manual, Version 6.11. Dassault Systèmes Simulia Corporation, Providence, Rhode Island, USA.

[2] Bischoff, P. H. and Perry, S. H. Compressive behaviour of concrete at high strain rates. *Materials and Structures*, Materiaux et Constructions (1991) 24:425-450.

[3] Carreira, D. J. and Chu, K. Stress strain relationship for plain concrete in compression. *ACI Journal*, November-December (1985) 82-72:797-804.

[4] Carreira, D. J. and Chu, K. Stress strain relationship for reinforced concrete in tension. *ACI Journal*, January-Febuary (1986) 83-3:21-28.

[5] Chakraborty, T., Larcher, M. and Gebbeken, N. Comparative performance of tunnel lining materials under blast loading. *3rd International Conference on Computational Methods in Tunnelling and Subsurface Engineering*, Ruhr University Bochum (2013).

[6] Chille, F., Sala, A. and Casadei, F. Containment of blast phenomena in underground electrical power plants. *Advances in Engineering Software* (1998) 29:7-12.

[7] Choi, S., Wang, J., Munfakh, G. and Dwyre, E. 3D nonlinear blast model analysis for underground structures. *GeoCongress 2006 ASCE* (2006):1-6.

[8] Du, H. and Li, Z. Numerical analysis of dynamic behaviour of rc slabs under blast loading. *Trans. Tianjin University* (2009) 15:061-064.

[9] Feldgun, V. R., Kochetkov, A. V., Karinski, Y. S. and Yankelevsky, D. Z. Internal blast loading in a buried lined tunnel. *International Journal of Impact Engineering* (2008) 35:172-183.

[10] Goel, M. D., Matsagar, V. A. and Gupta, A. K. Dynamic response of stiffened plates under air blast. *International Journal of Protective Structures* (2011) 2:139-155.

[11] Goel, M. D., Matsagar, V. A., Gupta, A. K. and Marburg, S. An abridged review of blast wave parameters. *Defence Science Journal* (2012) 62:300-306.

[12] Gui, M.W. and Chien, M. C. Blast resistant analysis for a tunnel passing beneath Taipei Shongsan airport - a parametric study. *Geotechnical and Geological Engineering* (2006) 24:227-248.

[13] Higgins, W., Chakraborty, T. and Basu, D. A high strain-rate constitutive model for sand and its application in finite element analysis of tunnels subjected to blast. *International Journal for Numerical and Analytical Methods in Geomechanics* (2012) 37:2590-2610.

[14] Johnson, G. R., and Cook, W. H. A constitutive model and data for metals subjected to large strains, high strain rates and high temperatures. Proceedings of *7th International Symposium on Ballistics Hague, Netherlands* (1983) 541-547.

[15] Liu, H. Dynamic analysis of subway structures under blast loading. *Geotechnical and Geological Engineering* (2009) 27:699-711.

[16] Lu, Y. Underground blast induced ground shock and its modelling using artificial neural network. *Computers and Geotechnics* (2005) 32:164-178.

[17] Lubliner, J., Oliver, J., Oller, S. and Onate, E. A plastic damage model for concrete. *International Journal of Solids and Structures* (1989) 25:299-329.

[18] Ngo, T. and Mendis, P. P. Modelling reinforced concrete structures subjected to impulsive loading using concrete lattice model. *Electronic Journal of Structural Engineering* (2008) 8:80-89.

[19] TM5-1300 Structures to resist the effects of accidental explosions. *US Departments of the Army and Navy and the Air Force* (1990).

[20] Veyera, G. E. and Ross, C. A. High strain rate testing of unsaturated sands using a split-hopkinson pressure bar. *3rd International Conference on Recent Advances in Geotechnical Earthquake Engineering and Soil Dynamics* (1995) 1.11.

[21] Zukas, J. A. and Walters, W. P. Explosive effects and applications. *Springer-Verlag New York, 1998* (2003).